A Telegrapher Equation for Electric Telemetering in Drill Strings

José M. Carcione and Flavio Poletto

***Abstract*—A reliable method of transmitting downhole information to the surface while drilling is essential to improve drilling applications. We have designed a numerical algorithm for simulation of electric-signal transmission through the drill string, based on the telegrapher equation (a circuit model). The drill string is then represented by a transmission line with varying geometrical and electromagnetic properties versus depth, depending on the characteristics of the drill string/formation system. These properties are implicitly modeled by the series impedance and the shunt admittance of the transmission line. The telegrapher equation is solved in the high-frequency range by using a direct method.**

***Index Terms*—Drill string, electric current, simulation, transmission line.**

I. Introduction

A KEY element in drill steering and prediction of lithology ahead-of-the-bit is the transmission of while-drilling information from the bottom of the well to the rig operator and the geophysicists. Systems for transmitting this information are diverse [3] and include: 1) mud logging, by which the returning mud stream is monitored for traces of formation gas; 2) cables through the drill string; 3) telemetering using radio waves and electromagnetic fields through the earth [12]; 4) telemetering by relay stations in the drill pipes; 5) telemetering by means of tracers in the mudstream; 6) storing the logging information in a retrievable recorder; 7) acoustic telemetering through the mudstream, through the drill string [10], [6], or through the earth (seismic telemetry), etc. An important application of the seismic telemetry method is the Seisbit technology, which uses the extensional wave generated at the drill bit (the pilot signals detected at the rig) to obtain RVSP seismograms [2].

Another possibility is the transmission of electric pulses through the drill string. This solution has the advantage of instantaneous synchronization of seismic data. The related problem has been studied since the 1970s. Hill and Wait [13] investigated the propagation of a signal from a toroidal coil source near the bottom of a drill rod to the surface. They predicted optimum frequencies in the 10–100 Hz range for depths of the order of several kilometers. The research indicated that, for depths of the order of 2 km and earth resistivities of the order of 100 Ωm, frequency effects become important at frequencies of several hertz. The same researchers [14], [19] suggested insulating the rod to decrease losses. Bhagwan and Trofimenkoff [4], [5] use a ladder network representation of the drill string. Their predictions agree with Hill and Wait's results for drill stem lengths in the 0.5-2.5 km range and in the frequency range from dc to about 1 kHz. This transmission line model appears, therefore, to be useful for system performance evaluation. DeGauque and Grudzinski [9], using electromagnetic theory, demonstrated that, because of the finite conductivity of the drill pipes, decreasing the frequency below a few hertz does not improve the communication. They also demonstrated that the attenuation coefficient becomes a constant below a given frequency and that decreasing the frequency does not increase the communication range, but, on the contrary, decreases the transmission rate. They obtained an optimum frequency corresponding to a minimum attenuation and a maximal data rate. Soulier and Lemaitre [17] favor the transmission line representation of the drill string, modeling the system as a coaxial cable acting as a waveguide. The main conductors are the casing and drill pipes; the shielding are the formations situated at infinity; and the insulation are the formations around the well. Using this model, they claim to obtain results that are consistent with field data. Recently, Xia and Chen [20] investigated the problem in the low-frequency range and obtained a good agreement between theoretical and experimental results. The frequency range of operation is essential, since high frequencies attenuate rapidly and low frequencies are not suitable to transmit information at a sufficient data rate.

In this paper, we develop a time-domain algorithm for the propagation of electric signal along the drill string. The method, based on the telegrapher equation, considers the presence of the coupling joints, nonuniform cross section areas, and varying drill string and formation electromagnetic properties. The approach is basically a version of the ladder-network or coaxial-cable representation. A fourth-order Runge–Kutta method and the Fourier differential operator are used to advance the solution in time and compute the spatial derivatives, respectively [6].

II. Electric-Transmission Differential Equation

A. Telegrapher Equation

Transmission of electric pulses through a drill string can be simulated by using a transmission line model. Consider a drill string connected between a source and a load. Within any short length we can define both energy storage and dissipation. The latter occurs both in the drill string and in the media surrounding the drill string. A cross section of the system and a circuit displaying these properties are shown in Fig. 1(a) and (b), respectively, where ρ, ϵ, and μ denote resistivity, permittivity, and mag-

Manuscript received July 18, 2001; revised January 16, 2002. This work was supported in part by AGIP SpA.

The authors are with the Istituto Nazionale di Oceanografia e di Geofisica Sperimentale (OGS), 34010 Sgonico, Trieste, Italy (e-mail: jcarcione@ogs.trieste.it).

Publisher Item Identifier S 0196-2892(02)04810-6.

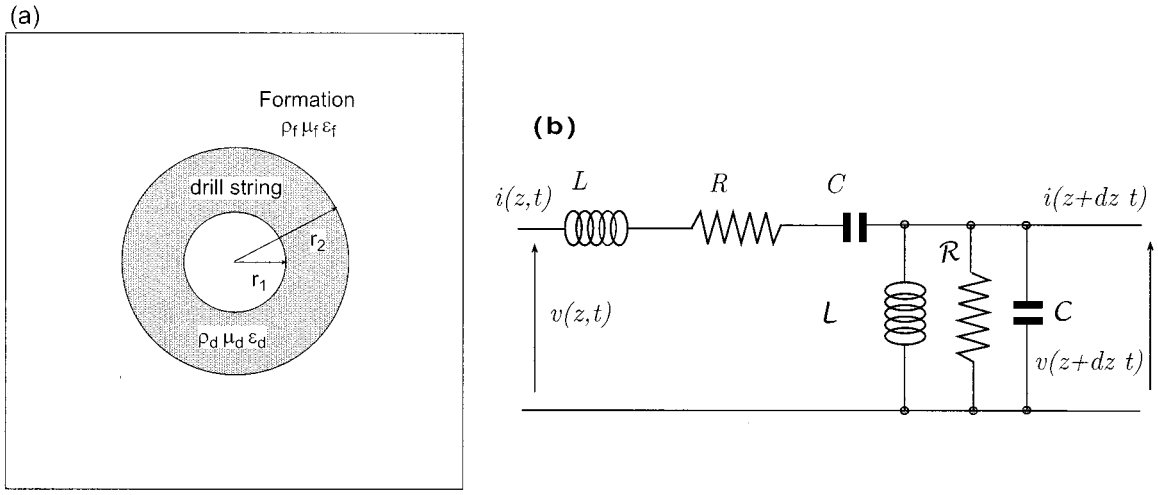

Fig. 1. (a) Section of drill string/formation system and (b) corresponding circuit representation where ρ, ϵ, and μ denote resistivity, permittivity, and magnetic permeability, respectively. The series- and shunt-inductance, capacitance and resistance, L, C, R, and $\mathcal{L}$, $\mathcal{C}$, $\mathcal{R}$ characterize the system. The circuit corresponds to a length δz of the transmission line. The voltage and current are functions of depth z and time t, so that the terminal conditions are those shown in (b), where v is the voltage and i is the electric current.

netic permeability, respectively. The series inductance L and resistance R, and shunt capacitance $\mathcal{C}$ are measured by unit length, and the series capacitance C and shunt resistance $\mathcal{R}$ and inductance $\mathcal{L}$ are measured per inverse of unit length (the inverse of $\mathcal{R}$ is the conductance per unit length). The circuit shown in Fig. 1(b) corresponds to a length δz of the line. The voltage and current are functions of depth z and time t, so that the terminal conditions are those shown in the figure, where v is the voltage and i is the electric current. Expressing the change in voltage $\delta v = v(z+dz, t) - v(z, t)$, and taking the limit $\delta z \to 0$, we have

$$\frac{\partial v}{\partial z} = -\left(Ri + L\frac{\partial i}{\partial t} + \frac{1}{C}\int i\,dt\right). \tag{1}$$

Similarly, summing the currents in the shunt elements implies

$$\frac{\partial i}{\partial z} = -\left(\frac{1}{\mathcal{R}}v + \mathcal{C}\frac{\partial v}{\partial t} + \frac{1}{\mathcal{L}}\int v\,dt\right). \tag{2}$$

Differentiating (1) with respect to z and (2) with respect to t, we obtain

$$\frac{\partial^2 v}{\partial z^2} = \left(\frac{R}{\mathcal{R}} + \frac{\mathcal{C}}{C} + \frac{L}{\mathcal{L}}\right)v + \left(R\mathcal{C} + \frac{L}{\mathcal{R}}\right)\frac{\partial v}{\partial t} + L\mathcal{C}\frac{\partial^2 v}{\partial t^2} + \left(\frac{R}{\mathcal{L}} + \frac{1}{C\mathcal{R}}\right)\int v\,dt + \frac{1}{C\mathcal{L}}\iint v\,dt\,dt'. \tag{3}$$

The standard telegrapher equation is obtained for $C \to \infty$ and $\mathcal{L} \to \infty$ [16]

$$\frac{\partial^2 v}{\partial z^2} = \frac{R}{\mathcal{R}}v + \left(R\mathcal{C} + \frac{L}{\mathcal{R}}\right)\frac{\partial v}{\partial t} + L\mathcal{C}\frac{\partial^2 v}{\partial t^2}. \tag{4}$$

The wave equation for lossless media is obtained for $\mathcal{R} \to \infty$ and $R \to 0$, i.e., no energy dissipation into the formation and a perfect conducting rod.

Equation (4) contains time integrals, which are expensive to evaluate with numerical methods. We recast the telegrapher equation in matrix form, thus avoiding these integrals. Defining the new variables

$$q = \int i\,dt \quad \text{and} \quad \varphi = \int v\,dt \tag{5}$$

and using (1) and (2), the telemetry equations can be written in matrix form as

$$\frac{\partial}{\partial t}\begin{pmatrix} i \\ v \\ q \\ \varphi \end{pmatrix} = -\begin{pmatrix} RL^{-1} & L^{-1}\partial_z & (LC)^{-1} & 0 \\ \mathcal{C}^{-1}\partial_z & (\mathcal{RC})^{-1} & 0 & (\mathcal{LC})^{-1} \\ -1 & 0 & 0 & 0 \\ 0 & -1 & 0 & 0 \end{pmatrix} \cdot \begin{pmatrix} i \\ v \\ q \\ \varphi \end{pmatrix} + \begin{pmatrix} i_s \\ v_s \\ 0 \\ 0 \end{pmatrix} \tag{6}$$

where ∂_z denotes spatial differentiation. Note that we have introduced the source terms i_s and v_s. Equation (6) is a generalization of the telegrapher's equation [18], [16], [8], since the coefficients may depend on the spatial variable z. This approach does not takes into account the propagation of the electric and magnetic fields, since it does not predict the set of waveguide modes [15], [18]. However, the distributed circuit approach does, in fact, give the correct description for the principal (TEM) wave. Moreover, it is more flexible than the electromagnetic approach, since the coefficients can be generalized to time-dependent functions, and the system is not constrained to be perfectly straight.

B. Parameters of the Drill String Formation System

Let us calculate the different parameters for the drill string illustrated in Fig. 1(a). The series resistance is

$$R = \rho_d/S = \rho_d/[\pi(r_2^2 - r_1^2)] \tag{7}$$

where S is the area and r_1 and r_2 are the inner and outer radii of the drill string, respectively.

The lateral area per unit length of drill string is $2\pi r_2$. If r is the radial variable, the shunt resistance is given by

$$\mathcal{R} = \int_{r_2}^{r_\infty} \frac{\rho_f}{2\pi r}\, dr = \frac{\rho_f}{2\pi} \ln\left(\frac{r_\infty}{r_2}\right) \tag{8}$$

where r_∞ is undetermined, but can be estimated using the fact that the drill string has a finite length. We approximate the drill string by half of a prolate ellipsoid of semilength l (the drill string length) and radius r_2 [5]. The shunt capacitance of the ellipsoid is [1], [4]

$$\begin{aligned}\mathcal{C}_e &= 4\pi\epsilon_f \sqrt{l^2 - r_2^2}\left[\ln\left(\frac{l+\sqrt{l^2-r_2^2}}{r_2}\right)\right]^{-1} \\ &\approx 4\pi\epsilon_f l\left[\ln\left(\frac{2l}{r_2}\right)\right]^{-1}\end{aligned} \tag{9}$$

where the approximation holds for a very long ellipsoid ($l \gg r_2$). The shunt capacitance $\mathcal{C}$ is obtained by dividing $\mathcal{C}_e$ by $2l$

$$\mathcal{C} = 2\pi\epsilon_f \left[\ln\left(\frac{2l}{r_2}\right)\right]^{-1}. \tag{10}$$

The shunt resistance is

$$\mathcal{R} = \frac{\rho_f \epsilon_f}{\mathcal{C}} = \frac{\rho_f}{2\pi} \ln\left(\frac{2l}{r_2}\right). \tag{11}$$

Comparing (8) and (11) yields $r_\infty = 2l$, the length of the drill string. Similarly, the series inductance is [5], [16]

$$L = \frac{\mu_f}{2\pi} \ln\left(\frac{2l}{r_2}\right). \tag{12}$$

We assume that the series capacitance of the drill pipes and coupling joints are equal to infinite, and that a finite capacitance C arises at the contact between the joints and the pipes. Similarly, the shunt inductance $\mathcal{L}$ is introduced on heuristic grounds. Both the shunt capacitance and inductance are used here as free parameters and should be calculated or measured.

Summarizing, the field variables and material properties with the corresponding units in the SI system are

$$\begin{array}{ll} v[\mathrm{V}] & i[\mathrm{A}] \\ R = \rho_d/S\ [\Omega/\mathrm{m}] & \mathcal{R} = \rho_f\gamma\ [\Omega\cdot\mathrm{m}] \\ L = \mu_f\gamma\ [\mathrm{H/m}] & \mathcal{L}[\mathrm{H}\cdot\mathrm{m}] \\ C[\mathrm{F}\cdot\mathrm{m}] & \mathcal{C} = \epsilon_f/\gamma\ [\mathrm{F/m}] \end{array} \tag{13}$$

where

$$\gamma = \frac{1}{2\pi} \ln\left(\frac{2l}{r_2}\right) \tag{14}$$

and 1 H = 1 V s/A, 1 F = 1 A s/V and 1 Ω = 1 V/A. The free space permittivity and magnetic permeability are $\epsilon_0 = 8.85 \times 10^{-12}$ F/m and $\mu_0 = 4\,\pi\,10^{-7}$ H/m, respectively.

Equation (6) is solved with a fourth-order Runge Kutta technique [7]. The spatial derivatives are calculated with the Fourier method by using the fast Fourier transform (FFT) [11]. This approximations is infinitely accurate for band-limited periodic functions with cutoff spatial wavenumbers which are smaller than the cutoff wavenumbers of the mesh.

III. Phase Velocity and Attenuation Factor

Let us assume a harmonic wave with a phase factor $\exp(\imath\omega t)$, where ω is the angular frequency and $\imath = \sqrt{-1}$. Then, (1) and (2) can be written as

$$\frac{\partial v}{\partial z} = \left(R + \imath\omega L + \frac{1}{\imath\omega C}\right) i \equiv Zi \tag{15}$$

and

$$\frac{\partial i}{\partial z} = \left(\frac{1}{\mathcal{R}} + \imath\omega\mathcal{C} + \frac{1}{\imath\omega\mathcal{L}}\right) v \equiv Yv \tag{16}$$

where Z and Y are the series impedance and the shunt admittance, respectively [18].

Now, assume a planewave with an spatial phase factor $\exp(-\imath\omega s z)$, where s is the complex slowness. The real and imaginary parts of s are related to the wavenumber and the attenuation, respectively. For any field variable, we have $\partial_z \rightarrow -\imath\omega s$. Eliminating the voltage and the current in (15) and (16) gives the dispersion equation

$$ZY + (\omega s)^2 = 0. \tag{17}$$

The phase velocity and attenuation factor are given by

$$V_p = [\mathrm{Re}\,(s)]^{-1} \quad \text{and} \quad \alpha = -\omega \mathrm{Im}(s) \tag{18}$$

respectively, with the operators Re and Im denoting real and imaginary parts, respectively.

IV. Examples

Wait and Hill's [19] solution for an infinitely long and lossless rod is

$$i(z) = \frac{2\pi K}{\eta}\left[\ln\left(-\frac{2\imath z}{\Gamma^2 r_2^2 k}\right)\right]^{-1} \exp(-\imath k z) \tag{19}$$

where

$$k = -\imath\sqrt{\imath\omega\mu_f(\sigma_f + \imath\omega\epsilon_f)} \quad \text{and} \quad \eta = \mu_f\omega/k \tag{20}$$

$\sigma_f = 1/\rho_f$ and Γ = 1.781. The effective magnetic current K in the source is proportional to frequency [13]. The normalization is such that $K = 1$ V at 5 kHz, i.e., $K = (f/5\ \mathrm{kHz})$ V, where $f = \omega/2\pi$ is the frequency.

Bhagwan and Trofimenkoff [5] take into account the boundary conditions at both ends of the string. Their solution for an ideal (lossless) rod of finite length l is

$$\begin{aligned} i(l) = 2\pi V_T \Big\{ k_0 \rho_f \cosh(k_0 l)\Big[\ln\left(\frac{2l}{r_2}\right)\tanh(k_0 l) \\ + \ln\left(\frac{\Delta l}{r_2}\right)\coth(k_0\Delta l)\Big]\Big\}^{-1} \end{aligned} \tag{21}$$

where $V_T = \omega/(10\,000\pi)$ V; Δl is the length of the downhole electrode ($\Delta l = 100$ m in these calculations); and

$$k_0 = \sqrt{\frac{\imath\omega\mu_f}{\rho_f}}. \tag{22}$$

The following are the parameters considered by Wait and Hill [19] and Bhagwan and Trofimenkoff [5]: $l = 1000$ m, $r_1 = 0$,

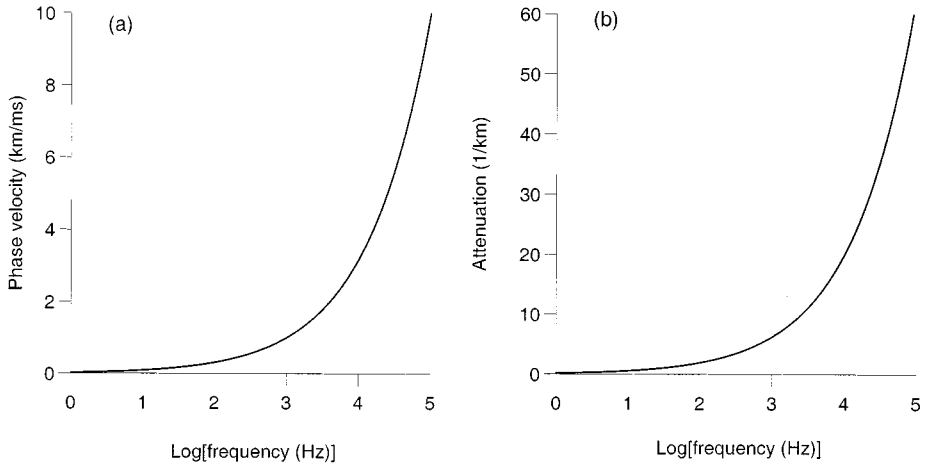

Fig. 2. (a) Phase velocity and (b) attenuation factor versus frequency for a perfectly conducting drill string. The parameters correspond to the example discussed by Wait and Hill [19].

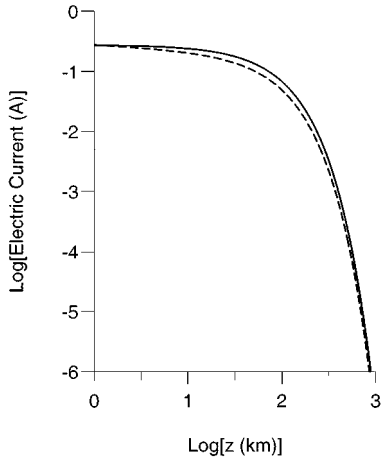

Fig. 3. Electric current versus distance on an infinitely long rod excited by a magnetic ring source for a frequency of 5 kHz. The continuous line is (27) and the broken line is Wait and Hill's solution [(19)]. Our curve is normalized to the value of Wait and Hill at 10 m.

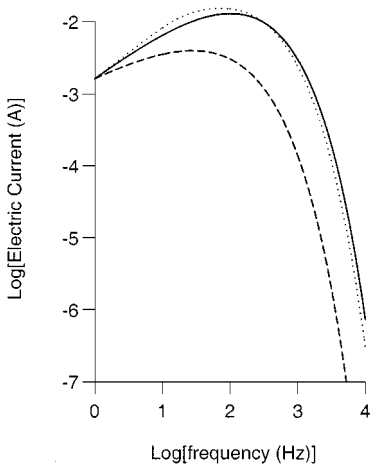

Fig. 4. Electric current versus frequency at $z = 1000$ m on a drill rod. The continuous line is (27), the broken line is Wait and Hill's solution [(19)], and the dashed line is Bhagwan and Trofimenkoff's solution, for a rod of finite dimensions. The curves are normalized to the value of Wait and Hill at 1 Hz.

$r_2 = 0.02$ m, $\rho_d = 0$, $\rho_f = 100\ \Omega\cdot$ m, $\mu_f = \mu_0$, and $\epsilon_f = 10\,\epsilon_0$. Moreover, $C = \infty$ and $\mathcal{L} = \infty$.

From (4) and (13), the differential equation associated with Wait and Hill's solution is

$$\frac{\partial^2 v}{\partial z^2} = L\left(\frac{1}{\mathcal{R}}\,\frac{\partial v}{\partial t} + \mathcal{C}\,\frac{\partial^2 v}{\partial t^2}\right) = \mu_f\left(\frac{1}{\rho_f}\,\frac{\partial v}{\partial t} + \epsilon_f\,\frac{\partial^2 v}{\partial t^2}\right). \tag{23}$$

If the formation is a perfect dielectric ($\rho_f \to \infty$), we obtain the wave equation, with the electromagnetic velocity of the formation equal to $1/\sqrt{\mu_f \epsilon_f}$. For a conducting formation, the frequency-domain solution takes a simple form. We obtain

$$ZY = \frac{i\omega\mu_f}{\rho_f} - \omega^2\mu_f\epsilon_f \tag{24}$$

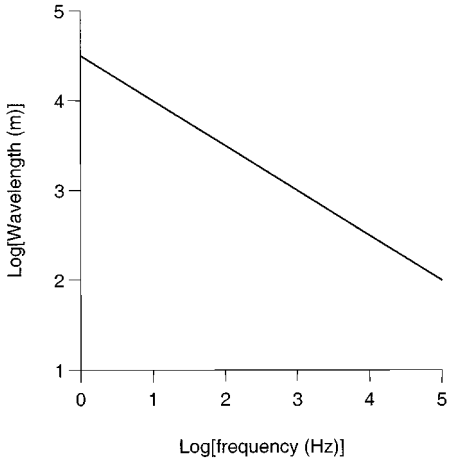

Fig. 5. Dominant wavelength of the signal transmitted through a rod.

where we have used (13). Because the second term in (24) is negligible for the values used by Wait and Hill [19] and for the

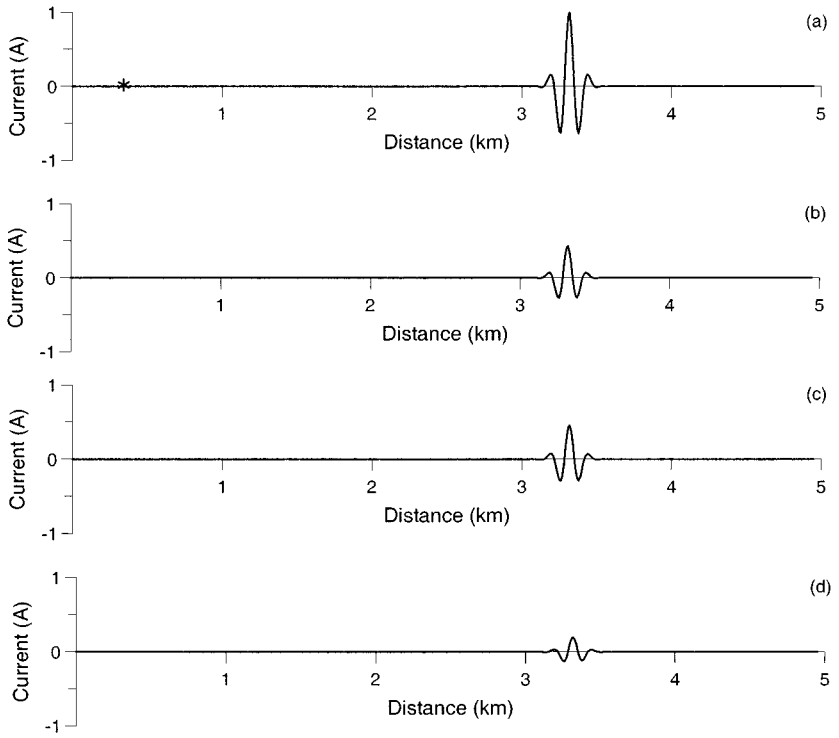

Fig. 6. Propagation of a pulse in a rod immersed in drilling fluid. Set of snapshots of the electric current at 24 μs, corresponding to different cases: (a) lossless rod and lossless fluid; (b) lossless rod and lossy fluid; (c) lossy rod and lossless fluid; and (d) lossy rod and lossy fluid. The asterisk indicates the location of the source.

frequency range under consideration, we obtain the following complex slowness from (17):

$$s = \sqrt{\frac{-\imath\mu_f}{\omega\rho_f}} = \frac{\imath k_0}{\omega}. \tag{25}$$

In the time-domain, this approximation corresponds to the diffusion equation

$$\frac{\partial^2 v}{\partial z^2} = \left(\frac{\mu_f}{\rho_f}\right)\frac{\partial v}{\partial t}. \tag{26}$$

Thus, the phase velocity and attenuation factor are simply

$$V_p = \sqrt{\frac{2\omega\rho_f}{\mu_f}} \quad \text{and} \quad \alpha = \sqrt{\frac{\omega\mu_f}{2\rho_f}} \tag{27}$$

since the propagation effects due to the finite length of the drill string have not been taken into account in our calculations, and the dielectric effects are negligible. Bhagwan and Trofimenkoff's phase velocity and attenuation factor coincides with ours if $l \rightarrow \infty$ in their equation [(17)]. The (a) phase velocity and (b) attenuation factor versus frequency are shown in Fig. 2. Phase velocity, and therefore data rates, increases with frequency, but attenuation also increases. The electric current associated with (27) is

$$i(z) = i_0 \exp(-\alpha z) \tag{28}$$

where $i_0 = (f/5\ \text{kHz})$ A, to be consistent with [13] and [19].

Fig. 3 shows the electric current versus distance on an infinitely long rod excited by a magnetic ring source for a frequency of 5 kHz. Fig. 4 represents the electric current versus frequency at a distance $z = 1000$ m from the source. The dashed line is Bhagwan and Trofimenkoff's attenuation curve for a rod of finite dimensions ($l = 1000$ m). The parameter γ in (14) is calculated by using $l = 1000$ m. The curves are normalized with respect to the lower frequency value of [19]. As can be inferred from Figs. 3 and 4, the magnitude of the excited current decays very rapidly after 0.5-km distance, and the current is weaker at higher frequencies. However, the velocity of transmitting signals decreases at low frequencies, as illustrated in Fig. 2(a). The group velocity is the derivative of the frequency with respect to the real wavenumber $\mathrm{Re}(\omega s)$

$$V_g = \frac{\partial\omega}{\partial \mathrm{Re}(\omega s)} = \left[\mathrm{Re}\left(\frac{\partial(\omega s)}{\partial\omega}\right)\right]^{-1}. \tag{29}$$

We obtain

$$V_g = \frac{2\rho_f}{\mu_f}\left[\mathrm{Re}\left(\frac{1}{k_0}\right)\right]^{-1} = 2V_p. \tag{30}$$

Thus, the dominant wavelength of a wave packet is given by

$$\lambda = \frac{2V_p}{f} = 4\pi\sqrt{\frac{2\rho_f}{\omega\mu_f}}. \tag{31}$$

The wavelength versus frequency is shown in Fig. 5. It ranges from 31.5 km at 1 Hz to 100 m at 100 kHz.

A. Simulations

The previous example corresponds to a diffusive field, since the electric displacement term [the second term in the right-hand side of (24)] is small compared to the conductivity term [the first term in the right-hand side of (24)]. Let us consider that the

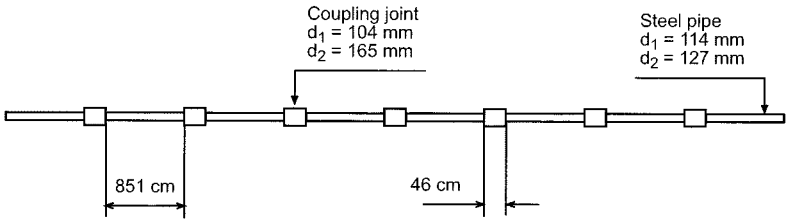

Fig. 7. Regular drill string consisting of pipes and tool joints.

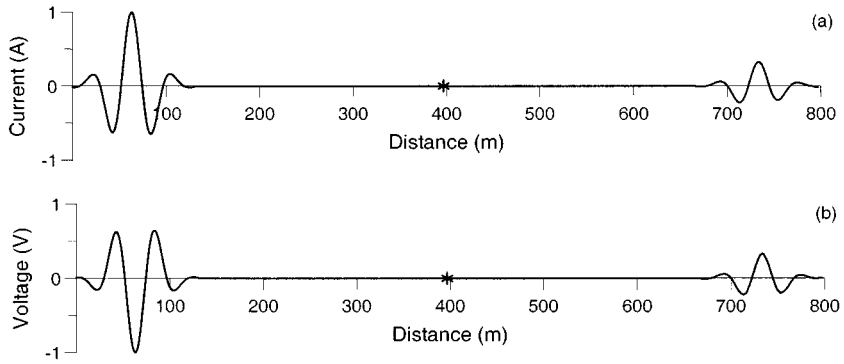

Fig. 8. Snapshots of the (a) current and (b) voltage at 3 μs propagation time. The asterisk indicates the location of the source.

rod is immersed in a dielectric fluid, such as oil-based drilling fluid, and assume the following properties: $l = 1000$ m, $r_1 = 0$, $r_2 = 0.02$ m, $\rho_d = 0.0002\ \Omega \cdot$ m, $\rho_f = 300\,000\ \Omega \cdot$ m, $\mu_f = \mu_0$, $\epsilon_f = 5\,\epsilon_0$, $C = \infty$, and $\mathcal{L} = \infty$. We consider $n_z = 495$ grid points and a uniform grid spacing $dz = 10$ m. The source central frequency is 1 MHz and is located at grid point 30. Absorbing strips of length 18 grid points are implemented at the two ends of the rod to avoid wrap-around effects. The wave field is computed by using a time-step of 20 ns.

Fig. 6 shows a set of snapshots of the electric current at 24 μs, corresponding to different cases: (a) lossless rod and lossless fluid, (b) lossless rod and lossy fluid, (c) lossy rod and lossless fluid, and (d) lossy rod and lossy fluid. The pulse has traveled approximately 3.2 km (from left to right), and has been attenuated by losses in both the fluid and the rod material.

The last example considers a drill string with the characteristics shown in Fig. 7, in a fluid the properties of which are those of the previous example. We assume a series capacitance $C = 10^9$ m$^2 \times C$ for the tool joints, to model capacitive effects between the pipes and the coupling joints. We consider $n_z = 3465$ and a uniform grid spacing $dz = 23$ cm. The source is located at grid point 1732 and has a central frequency of 3 MHz. The first half of the string has no tool joints. The first tool joint starts at grid point 1755, with each joint modeled by two grid points and each pipe element modeled by 37 grid points. The wave field is computed by using a time-step of 1 ns. Fig. 8 shows snapshots of the (a) current and (b) voltage at 3 μs. The attenuation of the pulse traveling to the right is evident. This effect is mainly due to the series capacitance.

V. Conclusions

We have developed a theoretical and numerical approach for modeling electromagnetic wave propagation in drill strings. The model corresponds to a generalized telegrapher equation, which reduces to a diffusion equation at low frequencies and to a hyperbolic (wave) equation at high frequencies. We have solved the wave equation including resistive and capacitive losses in the surrounding medium and drill string material. Modeling at low frequencies requires an algorithm for parabolic differential equations.

In this phase of the research, we intended to obtain a physically meaningful theoretical model. Use of this theory for practical industrial application is a further matter of research, from the numerical and experimental points of view. We are currently investigating the low-frequency numerical solution, the incorporation of boundary conditions to model the ends of the string, the inclusion of different media around the string (casing, cementation, etc.), and frequency effects of the series resistance of the rod and shunt capacitance of the formation. The series resistance can increase with frequency due to the skin effect ($R \propto \sqrt{\omega}$) and the presence of out-of-phase conduction currents, and the shunt capacitance must include dielectric losses in the formation.

References

[1] M. Abraham and R. Becker, *The Classical Theory of Electricity and Magnetism*. Glasgow, U.K.: Blackie, 1950.

[2] L. Aleotti, F. Poletto, F. Miranda, P. Corubolo, F. Abramo, and A. Craglietto, "Seismic while-drilling technology: Use and analysis of the drill-bit seismic source in a cross-hole survey," *Geophys. Prosp.*, vol. 47, pp. 25–39, 1999.

[3] J. J. Arps and J. L. Arps, "The subsurface telemetry problem—A practical solution," *J. Petr. Tech.*, pp. 487–493, May 1964.

[4] J. Bhagwan and F. N. Trofimenkoff, "Electric drill stem telemetry," *IEEE Trans. Geosci. Remote Sensing*, vol. GE-20, pp. 193–197, 1982.

[5] ——, "Drill stem resistance effects in electric telemetry links," *IEEE Trans. Geosci. Remote Sensing*, vol. GE-21, pp. 141–144, 1983.

[6] J. M. Carcione and F. Poletto, "Simulation of stress waves in attenuating drill strings, including piezoelectric sources and sensors," *J. Acoust. Soc. Amer.*, vol. 108, pp. 53–64, 2000.

[7] M. A. Celia and W. G. Gray, *Numerical Methods for Differential Equations: Fundamental Concepts for Scientific and Engineering Applications*. Englewood Cliffs, NJ: Prentice-Hall, 1992.
[8] J. L. Davis, *Wave Propagation in Electromagnetic Media*. New York: Springer-Verlag, 1990.
[9] P. DeGauque and R. Grudzinski, "Propagation of electromagnetic waves along a drillstring of finite conductivity," *SPE Drill. Eng.*, pp. 127–134, June 1987.
[10] D. S. Drumheller and S. D. Knudsen, "The propagation of sound waves in drill strings," *J. Acoust. Soc. Amer.*, vol. 97, pp. 2116–2125, 1995.
[11] B. Fornberg, *A Practical Guide to Pseudospectral Methods*. Cambridge, U.K.: Cambridge Univ. Press, 1996.
[12] W. Goodman, "A magnetic antenna system for steering tool communication," *Gas Research Institute Mag.*, 1999.
[13] D. A. Hill and J. R. Wait, "Electromagnetic basis of drill-rod telemetry," *Electron. Lett.*, vol. 14, pp. 532–533, 1978.
[14] ——, "Calculated admittance of an idealized drill rod antenna in a lossy medium," *IEEE Trans. Antennas Propagat.*, vol. AP-23, pp. 701–704, 1979.
[15] L. Page and N. I. Adams, *Electrodynamics*. New York: Van Nostrand, 1940.
[16] K. F. Sander and G. A. L. Reed, *Transmission and Propagation of Electromagnetic Waves*. Cambridge, U.K.: Cambridge Univ. Press, 1986.
[17] L. Soulier and M. Lemaitre, "E.M. MWD data transmission status and perspectives," in *Proc. SPE/IADC*, 1993, 25 686.
[18] J. A. Stratton, *Electromagnetic Theory*. New York: McGraw-Hill, 1941.
[19] J. R. Wait and D. A. Hill, "Theory of transmission of electromagnetic waves along a drill rod in conducting rock," *IEEE Trans. Geosci. Electron.*, vol. GE-17, pp. 21–24, 1979.
[20] M. Y. Xia and Z. Y. Chen, "Attenuation predictions at extremely low frequencies for measurement-while-drilling electromagnetic telemetry system," *IEEE Trans. Geosci. Remote Sensing*, vol. 31, pp. 1222–1228, 1993.

José M. Carcione, photograph and biography not available at the time of publication.

Flavio Poletto, photograph and biography not available at the time of publication.